THE JOURNAL OF PHYSICAL CHEMISTRY LETTERS
A JOURNAL OF THE AMERICAN CHEMICAL SOCIETY

pubs.acs.org/JPCL

Letter

Coherent Preparation of Highly Vibrating and Rotating D_2 Molecules

William E. Perreault, Haowen Zhou, Nandini Mukherjee,* and Richard N. Zare*

Cite This: J. Phys. Chem. Lett. 2022, 13, 4682−4687

Read Online

ACCESS | Metrics & More | Article Recommendations | Supporting Information

ABSTRACT: Highly vibrationally and rotationally excited hydrogen molecules are of immense interest for understanding and modeling the physics and chemistry of the cold interstellar medium. Using a sequence of two Stark-induced adiabatic Raman passages, we demonstrate the preparation of rotationally excited D_2 molecules in the fourth excited vibrational level within its ground electronic state. The nearly complete population transfer to the target state is confirmed by observing both the threshold behavior as a function of the laser power and the depletion of the intermediate level. The vibrational excitation reported here opens new possibilities in the study of the much debated four-center reaction between a pair of hydrogen molecules. Additionally, these rovibrationally excited molecules could be potentially used to generate the high-intensity D^- ion beams considered essential for D−T thermonuclear fusion by enhancing the cross section for dissociative electron attachment by 5 orders of magnitude compared to that of the ground state.

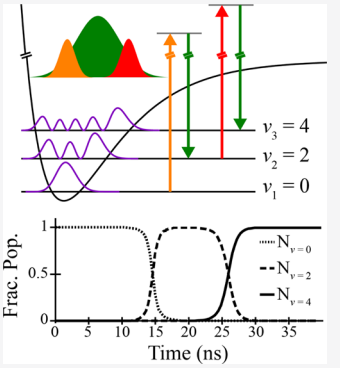

The collision dynamics of highly vibrationally excited H_2 molecules are immensely important to the physics and chemistry of the cold interstellar medium.[1−3] Additionally, low-energy scattering of H_2 molecules is an ideal experimental test bed for fundamental quantum collision theory, as the theoretical tractability of H_2 allows for direct comparison with calculations.[4−9] In these low-energy collisions, vibrational excitation is an excellent tool for interrogating the long-range van der Waals forces because these forces are sensitive to the molecular bond length. In cold chemistry, highly vibrationally excited states provide the energy to overcome the barrier to reaction. To obtain a good signal-to-noise ratio in an experiment involving cold collisions, which might have a small collision cross section, we need to prepare a large population in a targeted highly vibrationally excited state. Additionally, the weak long-range molecular forces are anisotropic, so collisions at low energies are highly sensitive to the relative orientations of the colliding species. Therefore, selecting a specific rotational state and its projection on a space-fixed axis, which defines the orientation of the quantum object, is another essential criterion for experiments studying cold collisions.

Many methods for preparing quantum states of molecular systems have been developed.[10−17] However, the preparation of H_2 molecules in a highly vibrationally and rotationally (rovibrational) excited quantum state is particularly challenging. This is because the homonuclear symmetry forbids dipole-allowed infrared excitation, and the weak two-photon Raman coupling between the initial and target vibrational states requires large optical powers that dynamically shift the Raman resonance. This dynamic Stark shift severely limits the efficiency of traditional Raman pumping. To overcome this limitation, we developed a technique called Stark-induced adiabatic Raman passage (SARP).[18] SARP is an off-resonant Raman excitation that consists of a pair of delayed but partially overlapping nanosecond laser pulses of unequal intensities. The dynamic Stark shift from the stronger laser pulse creates crossings of the light-induced adiabatic dressed states, and population transfer is achieved when one of the crossings becomes avoided. A comprehensive description of the SARP process is given in the Supporting Information as well as in our earlier publications.[19,20] Using SARP, we have demonstrated the preparation of a variety of vibrationally excited (v = 1, 2, 4, and 7) states of molecular hydrogen and its isotopologues in various specific rotational states (j = 0, 1, 2, and 3), where v and j represent the quantum numbers of vibrational and rotational energy levels, respectively.[19−22] Here, we use (v, j) to label rovibrational eigenstates, although in the language of spectroscopy they would be called levels.

However, the problems of a large dynamic Stark shift and weak coupling become more problematic for SARP to overcome for larger steps up the vibrational ladder. As illustrated in Figure 1A, when the vibrational quantum number v_2 of the target state is very different from that of the initial state, overlap of the initial and target vibrational wave functions is reduced, resulting in a smaller transition probability. The two-photon transition rate is determined by the Raman coupling, which is given by the relationship $\Omega \propto \mu_{v_1 v'} \mu_{v' v_2}$,

Received: April 22, 2022
Accepted: May 19, 2022

https://doi.org/10.1021/acs.jpclett.2c01209
J. Phys. Chem. Lett. 2022, 13, 4682−4687

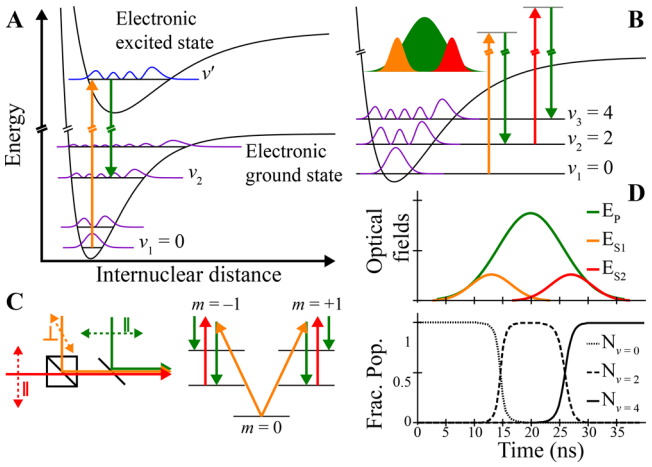

Figure 1. Two-step SARP process. (A) Raman excitation schematic, showing the wave functions of the initial and final states connected via an electronically excited vibronic state. Panel A shows a resonant Raman transition for ease of illustration, but the SARP processes in this work involve off-resonant Raman transitions with virtual electronically excited vibronic states. The overlap between the initial and final vibrational levels decreases with an increase in the change in the vibrational quantum number. (B) Schematic of the two-step SARP process described in this paper. D_2 molecules are excited from the ($v = 0$) ground state to the ($v = 4$) target state using a sequence of two SARP processes that drives population through a real intermediate ($v = 2$) state. The inset shows the temporal pulse sequence, with a stronger Stokes pulse (green) partially overlapping with two weaker pump pulses (orange and red). (C) Experimental arrangement for the combination of the three laser pulses. The two pump pulses are combined using a polarizing cube, requiring that their polarizations be perpendicular to one another. As shown in the schematic, this produces the ($m = \pm 1$) state. (D) Theoretical simulation of the two-step SARP process shows the possibility of transferring the complete population to the final state, with no population left stranded in the intermediate state.

where $\mu_{v_1 v'}$ and $\mu_{v' v_2}$ are the transition dipole moments connecting the initial v_1 and target v_2 states via the electronically excited vibronic state v'. Additionally, Stark detuning Δ, determined by the difference in the polarizabilities of the initial and target states, increases as the difference between v_1 and v_2 becomes larger, making dynamic detuning stronger. To achieve successful population transfer, the sweeping rate of the Stark-induced detuning must be sufficiently slow as defined by the Landau−Zener condition of adiabaticity: $d\Delta/dt < 4\Omega^2$.[19,20] As such, for transitions in which the difference in vibrational quantum numbers between the initial and target state is large, a single SARP step is very limited in its capability to transfer population. We have seen this concretely in our work on preparing the ($v = 7$) vibrational state where SARP's adiabaticity condition can be maintained over only a very small volume, resulting in a small target size that we found entirely impractical to use in our cold scattering experiments. Additionally, it was impossible to prepare any rotationally excited levels in either of the highly vibrationally excited states we have prepared previously ($v = 4$ or 7) because the large dynamic Stark shift of the rotationally aligned molecule breaks the adiabaticity condition.

What appears to be impossible to achieve using a single adiabatic transition, however, can be accomplished using multiple steps of adiabatic processes, each fulfilling the condition of adiabaticity to achieve a large target population. Using the multistep SARP process[23] with a strong Stokes pulse partially overlapping with a set of weaker pump pulses (Figure 1B), we have theoretically shown the possibility of preparing a scattering sensitive population in a highly excited vibrational state close to dissociation. For each smaller Δv SARP step, the adiabaticity condition is easily fulfilled because of the strong Raman coupling that results from the superior overlap of the vibrational wave functions. We have shown theoretically that two- and three-step SARP processes can prepare very highly vibrationally excited states of H_2. As illustrated in the simulation of two-step SARP in Figure 1D, at the end of excitation complete population of the initial state (v_1) is transferred to the target state (v_3), leaving no population in the intermediate SARP state (v_2). To experimentally demonstrate the idea, we carried out a two-step SARP process preparing two rovibrationally excited states D_2 ($v = 4$, $j = 2$) and ($v = 4$, $j = 4$). The two sequential SARP steps are connected via the intermediate ($v = 2$, $j = 2$) SARP state. The nearly complete population transfer from the initial ($v = 0$, $j = 0$) state to either of the target states is demonstrated by the threshold behavior of the measured target population against the fluence of the pump lasers, which is a hallmark of adiabatic passage. The complete population transfer is further supported by measuring the depletion of the population in the intermediate ($v = 2$) state. Additionally, we demonstrate the correlation between the saturation of the SARP population transfer to the target state and the nearly complete depletion of the initial state.

We estimate that a total population of $\sim 10^{10}$ deuterium molecules was prepared in the rovibrationally excited target states. The preparation of a dense sample of highly vibrationally excited and rotationally aligned D_2 molecules has important applications in solving long-standing problems in chemistry and physics. First, this preparation opens the possibility of investigating poorly understood four-center reactions like HD + HD → H_2 + D_2.[24−27] Excitation of the reactants to the ($v = 4$) level will help overcome the reaction barrier so that the reaction products can be probed at very low collision energies, which will give us better insight into their fundamental dynamics. Additionally, the high density of highly rovibrationally excited D_2 molecules could have important applications in D−T nuclear fusion. It has previously been shown that rotationally excited D_2 molecules at the ($v = 4$) level resonantly enhance the cross section for the resonant capture of a low-energy electron to generate D^- ions by at least 5 orders of magnitude.[28,29] As such, the preparation of a high density of highly excited D_2 molecules might be an important step toward generating bright D^- beams, which are considered essential for igniting and sustaining thermonuclear fusion.

We demonstrate here the preparation of highly rovibrationally excited states of D_2 molecules that have been expanded and collimated into a supersonic beam. Specifically, we use the two-step SARP process to transfer nearly the complete ($v = 0$, $j = 0$) ground state population of the D_2 molecular beam to the desired D_2 ($v = 4$, $j = 2$) or D_2 ($v = 4$, $j = 4$) target state. To create this two-step SARP, we combine a strong Stokes pulse (1064 nm, 10 ns) with a pair of weaker and delayed pump pulses (655 and 660−680 nm, 5 ns) as illustrated in Figure 1B. The single-mode pump pulses are derived from two seeded pulsed dye amplifiers (Sirah PulsAmp 5X-N), and the 1064 nm Stokes pulse is derived from an injection-seeded Nd^{3+}:YAG laser (Spectra Physics PRO 290). With respect to the Stokes pulse, the first pump pulse delay is controlled electronically while the second pump pulse delay is controlled using an

https://doi.org/10.1021/acs.jpclett.2c01209
J. Phys. Chem. Lett. 2022, 13, 4682−4687

optical delay line because the amplifier that produces it is pumped by the same YAG laser that generates the Stokes pulse. The laser beams are introduced into the molecular beam vacuum chamber and intersect the molecular beam transversely. The pump laser wavelength for the first SARP step is set to 655 nm to connect the ($v = 0$, $j = 0$) ground state to the ($v = 2$, $j = 2$) intermediate state, while the wavelength of the pump pulse for the second step is tuned to the Raman resonance connecting the intermediate to the target state: 660 nm for ($v = 4$, $j = 2$) and 676 nm for ($v = 4$, $j = 4$). Figure 1B shows the excitation schematic of the three-color double SARP used in our experiment to prepare the ($v = 4$) state.

The polarizations of the two pump laser beams must be crossed (Figure 1C) because they can be combined only using a polarizing beam splitter due to the relatively small difference in their wavelengths. The 1064 nm Stokes polarization can be parallel to either of the pump pulses because the pump pulses are combined with the Stokes pulse on a chromatic beam combiner that retains the polarizations of all three beams. SARP is most efficient when the transition being pumped has a small Stark shift and a strong Raman coupling. To that end, we have chosen to minimize the dynamic Stark shift of the second SARP transition by setting the polarization of the second pump to be parallel to the Stokes pulse, meaning that the first pump polarization is perpendicular to both. With this choice of pump and Stokes polarizations, the double SARP moves through intermediate state D_2 ($v = 2$, $j = 2$, $m = \pm 1$), where the m quantum number gives the projection of the internal angular momentum on a chosen quantization axis. We choose the polarization direction of the Stokes pulse as the quantization Z-axis for the projection quantum number.

Following beam combination, the pulses are focused onto the molecular beam using a 50 cm focal length lens. The focused spot of the Stokes laser has a diameter of 60 μm, whereas the focused diameters of the first and second pump lasers are 30 and 40 μm, respectively. Collimators placed in each beam path enabled us to bring the focus spots of all three laser beams within the molecular beam and optimize the overlap among the different laser beams. The D_2 molecules in the supersonic beam are moving at a speed of 2 μm/ns. Following the first SARP step, the vibrationally excited D_2 ($v = 2$) molecules will drift along the molecular beam before they are excited to the ($v = 4$) target state by the second SARP step. Therefore, to optimize the second SARP step, we needed to slightly spatially displace (by ~10 μm) the first and second pump lasers. The Stokes spot size was set larger than the two pump beams to enable this displacement while overlapping both pump beams with the Stokes laser. The populations in the intermediate ($v = 2$) and target ($v = 4$) states were detected state-selectively using (2+1) resonance-enhanced multiphoton ionization (REMPI). The REMPI signals from the intermediate and target states, which were generated by two independent ultraviolet (UV) laser sources, are proportional to the population of the ionized state.

Successful preparation of a large number of molecules in the highly vibrationally excited state requires efficient transfer from the ground state to the D_2 ($v = 2$, $j = 2$) intermediate state via the first SARP step. We have previously studied the SARP preparation of D_2 ($v = 2$, $j = 2$, $m = 0$) at length,[20] but here the intermediate state is D_2 ($v = 2$, $j = 2$, $m = \pm 1$); therefore, we have briefly revisited the optimization of this transition. Figure 2 shows the REMPI signal from the D_2 ($v = 2$, $j = 2$, $m = \pm 1$) intermediate state as a function of the Raman detuning at various pump-to-Stokes delays. The asymmetry in the observed spectra arises because of the dynamic Stark effect, which red shifts the Raman transition. Figure 2 clearly shows that SARP population transfer to the ($v = 2$) state is minimum at zero delay and increases at larger delays, which is counterintuitive and is a hallmark of SARP. As we detail in the Supporting Information, more than one crossing becomes avoided close to zero delay in the presence of a non-zero two-photon Rabi frequency. As a result, population that is transferred at the first crossing is returned at the second crossing. At very large delays, the two-photon Rabi frequency becomes too weak to maintain adiabaticity. Figure 2 shows that the optimum population transfer to the intermediate state is obtained at a pump-to-Stokes delay between 5 and 7 ns. As such, for the rest of the experimental data presented herein, the pump-to-Stokes delay of both SARP steps was held at 6 ns.

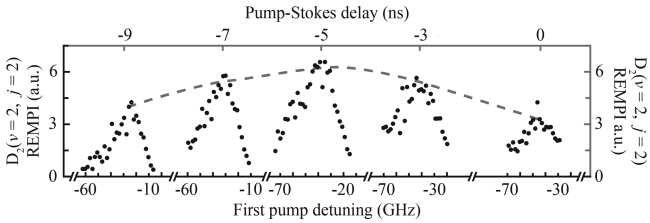

Figure 2. Spectra of the first SARP step D_2 ($v = 0$, $j = 0$) → D_2 ($v = 2$, $j = 2$, $m = \pm 1$) as a function of the delay between the first pump and Stokes pulse with the power of both pulses held constant. Experimental data clearly show that the population transfer is most efficient at a longer pump-to-Stokes delay of 5−6 ns. As the delay approaches zero, population transfer becomes less efficient because of the presence of multiple avoided crossings, resulting in coherent return and population oscillations. A detailed explanation of this behavior is given in the Supporting Information.

Figure 3A shows the (2+1) REMPI signal from the final ($v = 4$, $j = 2$, $m = \pm 1$) target state as the Raman detuning of the second SARP step is varied while the fluence of the second pump laser near 676 nm is held fixed at several values. For this measurement, the fluence of the Stokes and first pump lasers and the Raman detuning of the first SARP step were held at the values corresponding to the maximum of the REMPI signal from the intermediate ($v = 2$) level shown in Figure 2. Figure 3A shows the frequency shift and saturation of the maximum population transfer against the fluence of the second pump. The saturation occurs because SARP is a threshold phenomenon where adiabatic population transfer requires a minimum value of the two-photon Rabi frequency to satisfy the Landau−Zener condition. Figure 3A also shows the broadening of the spectrum with an increase in laser power. With an increase in laser fluence, adiabaticity is fulfilled over a broader range of the initial detuning, effectively shifting and widening the SARP spectrum.

Figure 3B shows the change in the REMPI signal from the intermediate D_2 ($v = 2$, $j = 2$, $m = \pm 1$) state as a function of the ($v = 2$) → ($v = 4$) Raman detuning at the various fluences of the second pump laser. Figure 3B shows a measurement of ~90% reduction of the intermediate state at the highest second pump laser fluence. This reduction represents nearly complete depletion of the intermediate state population as it is transferred to the final target state. This is a very significant achievement given the sensitivity of our measurement to the overlap of four separate pulsed laser beams at the micrometer scale. Thus, this confirms that we have achieved nearly

https://doi.org/10.1021/acs.jpclett.2c01209
J. Phys. Chem. Lett. 2022, 13, 4682−4687

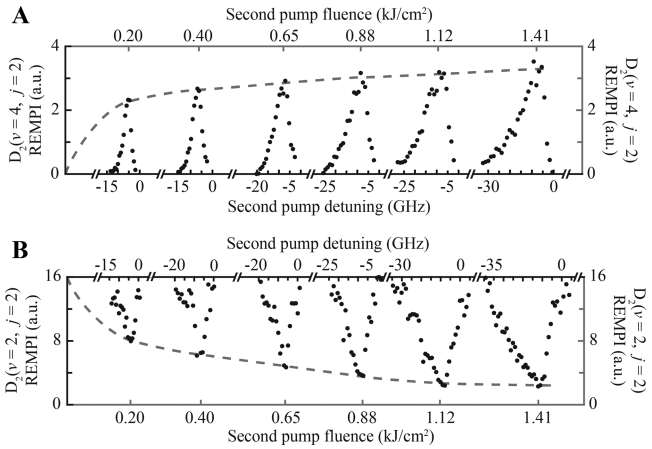

Figure 3. Spectra of the second SARP step D_2 ($v = 2$, $j = 2$, $m = \pm1$) → D_2 ($v = 4$, $j = 2$, $m = \pm1$) as a function of the second pump laser fluence. The fluence and frequency of the first pump are held constant at the values corresponding to the maximum population transfer shown in Figure 2. (A) Measured D_2 ($v = 4$, $j = 2$) target state REMPI signal. The saturation behavior of the signal with an increase in pump fluence shows the threshold characteristic of the SARP process, demonstrating that the complete population transfer is achieved as long as the two-photon coupling is sufficiently strong to satisfy the adiabatic condition. (B) Depletion of the REMPI signal from the D_2 ($v = 2$, $j = 2$) intermediate state confirms complete population transfer. Approximately 90% of the intermediate state molecules are pumped into the excited state within the measured REMPI volume.

complete population transfer to the ($v = 4$, $j = 2$, $m = \pm1$) target state. Additionally, if we compare the spectra in Figure 3B to those in Figure 3A, we can see that the depletion mirrors the saturation of the ($v = 4$, $j = 2$, $m = \pm1$) target state. This measurement thus proves that the characteristic saturation behavior of the SARP process indicates complete population transfer.

Figure 4 shows the (2+1) REMPI signal from the final ($v = 4$, $j = 4$, $m = \pm1$) target state at various fluences of the second

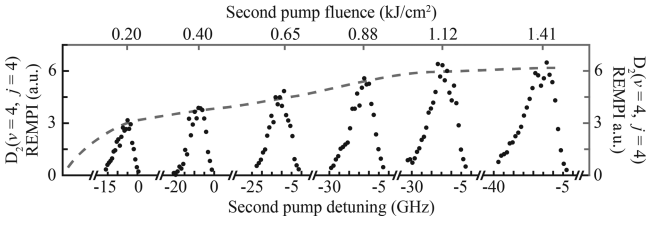

Figure 4. Spectra of the second SARP step D_2 ($v = 2$, $j = 2$, $m = \pm1$) → D_2 ($v = 4$, $j = 4$, $m = \pm1$) as a function of the second pump laser fluence. The fluence and frequency of the first pump are held constant at the values corresponding to the maximum population transfer shown in Figure 2. As in Figure 3, the saturation behavior demonstrates that complete population transfer is achieved within the REMPI volume. As we note in the text, the dynamic Stark shift from this transition is larger than the transition to D_2 ($v = 4$, $j = 2$, $m = \pm1$), so the adiabatic condition can be satisfied only within a smaller volume. As a result, we were unable to measure the depletion of the intermediate state for this transition.

pump laser. For this measurement, the Stokes and the first pump lasers were set to maximize the transfer to the intermediate ($v = 2$) state as in Figure 3. The saturation of the peak REMPI signal against the laser fluence again shows the characteristic threshold behavior, demonstrating nearly complete population transfer to the target state. However, we were unable to capture depletion of the intermediate ($v = 2$, $j = 2$) state for the preparation of this target state. We believe the failure to capture depletion is caused by the difficulty in aligning the second pump and REMPI UV laser relative to the first pump and Stokes lasers within the somewhat smaller volume prepared in this transition as compared to the ($v = 4$, $j = 2$) target state. We note that the dynamic Stark shift of the second SARP transition to the ($v = 4$, $j = 4$) state via the intermediate ($v = 2$, $j = 2$) state is appreciably larger than that experienced during preparation of the ($v = 4$, $j = 2$) target state via the same intermediate state. As a result, the adiabatic condition for the SARP transition to the ($v = 4$, $j = 4$) state is likely satisfied within a somewhat smaller volume, making it more difficult to locate. From a careful comparison of the REMPI signal generated by the ($v = 4$, $j = 4$) and ($v = 4$, $j = 2$) states using the same UV laser fluence, we estimate that the excited volume of the ($v = 4$, $j = 4$) target state is reduced to 30−40% of the volume of the ($v = 4$, $j = 2$) target state.

We note that the weaker pump pulses are placed symmetrically having positive and negative delays of 6 ns with respect to the center of the stronger pulse. This arrangement requires the lifetime of the intermediate ($v = 2$) state to be longer than the operation time of multistep SARP (~20 ns). This method can therefore be applied to excite states having a minimum lifetime of a few tens of nanoseconds. Although we have conducted these experiments in a supersonic beam, this multistep SARP process is equally applicable in a gas cell or even in the condensed phase as long as it meets this condition. Our earlier theoretical work suggested that multistep SARP also works with the weaker pulses added together on the same side as that of the stronger pulse.[23] We have explored this possibility experimentally. However, we found that the Stark shift from the overlapping weaker pulses changed too substantially the crossing of the adiabatic states, making it difficult to achieve consistent population transfer in both SARP steps.

We have demonstrated the preparation of two distinct rovibronic ($v = 4$, $j = 2$) and ($v = 4$, $j = 4$) states of the D_2 molecule using a two-step SARP process involving a single Stokes pulse partially overlapping with two weaker and delayed pump laser pulses. These rotationally aligned, highly stretched molecules open new avenues to study anisotropic interactions and the formation of resonant complexes in cold collisions in a completely field-free environment. We have previously prepared $H_2/D_2/HD$ molecules in ($j = 2$) rotational states within the ($v = 1$) and ($v = 2$) vibrational levels and used them in cold scattering experiments to interrogate the anisotropic van der Waals forces that influence dynamic resonances.[30−32] Because the molecular axis distribution in the highly spinning ($j = 4$) state is more sharply defined, it provides a higher level of precision in the control of the collision geometry. The double-SARP process described here is not limited to molecular hydrogen or its isotopologues. The method applies to the vibrational excitations of other molecules such as N_2, CO_2, C_2H_2, CH_4, etc., as long as the lifetime of the intermediate SARP state is longer than the SARP operation time (~20 ns). Additionally, by adding more than two SARP steps, we can reach vibrationally excited states close to the dissociation limit, thereby creating a pair of entangled atoms and opening the possibility of probing fundamental quantum effects in reactions. State preparation is an essential experimental tool for further understanding the fundamental

https://doi.org/10.1021/acs.jpclett.2c01209
J. Phys. Chem. Lett. 2022, 13, 4682−4687

mechanisms that govern chemical reaction processes. In particular, the preparation of the (v = 4) state may help enable fundamental studies of the long studied and poorly understood four-center reaction, HD (v = 4) + HD (v = 4) → H_2 + D_2, which continues to draw interest among experimentalists and theoreticians alike. Excitation to the (v = 4) state could provide the energy necessary to overcome the reaction barrier, and appropriate alignment of the reagents could control the barrier height, thus opening many new possibilities for exploring this interaction in the cold collision regime.

In addition, the D_2 (v = 4, j = 4) molecules can be used to generate high-intensity D^- beams via resonant collision with a low-energy electron beam. The theoretical work of Wadhera and Bardsley,[28] and others[33−35] suggested that the non-adiabatic crossings of the two interaction potentials D(1s) + D(1s) + e and $D^-(1s^2)$ + D(1s) can be utilized to resonantly capture a low-energy electron, which then dissociates producing D^-, a process known as dissociative electron attachment (DEA). The theoretical calculations were verified by the experimental work of Allan and Wong using both H_2 and D_2.[29,36] The combined experimental and theoretical work confirms that the DEA cross section for D_2 increases by nearly 5 orders of magnitude when the D_2 molecule is excited from the (v = 0) state to the (v = 4) state and also demonstrates that it is further enhanced by rotational excitation. High-intensity D^- ion beams are considered essential for igniting and heating a D−T thermonuclear fusion reaction (ITER).[37,38]

To apply this in an actual fusion reactor requires a flux of ∼10^{21} s^{-1} vibrationally excited D_2.[39] To show the applicability of SARP to this real-world problem, we suggest a method by which our production could be scaled up to approximately the rate required. The required laser fluence for SARP (∼25 J/mm^2) could be realized using a laser beam diameter of ∼1 cm for a laser output power of ∼2 kJ/pulse, which can be easily achieved using current laser technology. High-density (∼10^{19} molecules cm^{-3}) molecular beams with path lengths of a few centimeters have already been realized.[40,41] In this collision-free ambience, SARP could utilize longer single-mode laser pulses, making the higher powers more achievable and SARP more efficient. Combining these already-existing technologies would allow the generation of vibrationally excited (v = 4) pure D_2 molecules at a rate of >10^{20} molecules s^{-1}. Thus, we suggest that the SARP preparation of highly vibrationally and rotationally excited D_2 molecules might have practical importance.

■ ASSOCIATED CONTENT

Supporting Information

The Supporting Information is available free of charge at https://pubs.acs.org/doi/10.1021/acs.jpclett.2c01209.

Detailed description of the physics of the SARP process (PDF)

Transparent Peer Review report available (PDF)

■ AUTHOR INFORMATION

Corresponding Authors

Nandini Mukherjee − *Department of Chemistry, Stanford, California 94305, United States*; Email: nmukherj@stanford.edu

Richard N. Zare − *Department of Chemistry, Stanford, California 94305, United States*; orcid.org/0000-0001-5266-4253; Email: zare@stanford.edu

Authors

William E. Perreault − *Department of Chemistry, Stanford, California 94305, United States*

Haowen Zhou − *Department of Chemistry, Stanford, California 94305, United States*

Complete contact information is available at: https://pubs.acs.org/10.1021/acs.jpclett.2c01209

Notes

The authors declare no competing financial interest.

■ ACKNOWLEDGMENTS

This work was supported by the U.S. Army Research Office through the MURI program under Grant W911NF-19-1-0283 and National Science Foundation Grant PHY- 2110256.

■ REFERENCES

(1) Agúndez, M.; Goicoechea, J. R.; Cernicharo, J.; Faure, A.; Roueff, E. The Chemistry of Vibrationally Excited H_2 in the Interstellar Medium. *Astrophys. J.* **2010**, *713* (1), 662−670.

(2) Roueff, E.; Lique, F. Molecular Excitation in the Interstellar Medium: Recent Advances in Collisional, Radiative, and Chemical Processes. *Chem. Rev.* **2013**, *113* (12), 8906−8938.

(3) Gnaciński, P. Interstellar H_2 toward HD 147888. *Astron. Astrophys.* **2012**, *549*, 1−8.

(4) Sultanov, R. A.; Guster, D.; Adhikari, S. K. Low Temperature HD + Ortho-/Para-H_2 Inelastic Scattering of Astrophysical Interest. *J. Phys. B At. Mol. Opt. Phys.* **2016**, *49*, 015203.

(5) Veselinova, A.; Agundez, M.; Goicoechea, J. R.; Menendez, M.; Zanchet, A.; Verdasco, E.; Jambrina, P. G.; Aoiz, F. J. Quantum Study of Reaction O (3P) + H_2 (v,j) → OH + H: OH Formation in Strongly UV-Irradiated Gas. *Astron. Astrophys.* **2021**, *648*, A76.

(6) Schaefer, J.; Meyer, W. Theoretical Studies of H_2-H_2 Collisions. I. Elastic Scattering of Ground State Para- and Ortho-H_2 in the Rigid Rotor Approximation. *J. Chem. Phys.* **1979**, *70* (1), 344−360.

(7) Johnson, D. L.; Grace, R. S.; Skofronick, J. G. The Total Scattering Cross Sections for H_2 + H_2, D_2 + D_2, and HD + HD for Relative Collision Energies below 10 MeV. *J. Chem. Phys.* **1979**, *71* (11), 4554−4569.

(8) Simbotin, I.; Ghosal, S.; Côté, R. A Case Study in Ultracold Reactive Scattering: D + H_2. *Phys. Chem. Chem. Phys.* **2011**, *13* (42), 19148−19155.

(9) Martí, C.; Laganà, A.; Pacifici, L.; Pirani, F.; Coletti, C. A Quantum-Classical Study of the Effect of the Long Range Tail of the Potential on Reactive and Inelastic OH + H_2 Dynamics. *Chem. Phys. Lett.* **2021**, *769*, 138404.

(10) Gaubatz, U.; Rudecki, P.; Schiemann, S.; Bergmann, K. Population Transfer between Molecular Vibrational Levels by Stimulated Raman Scattering with Partially Overlapping Laser Fields. A New Concept and Experimental Results. *J. Chem. Phys.* **1990**, *92* (9), 5363.

(11) Halfmann, T.; Bergmann, K. Coherent Population Transfer and Dark Resonances in SO_2. *J. Chem. Phys.* **1996**, *104*, 7068−7072.

(12) Kuhn, A.; Steuerwald, S.; Bergmann, K. Coherent Population Transfer in NO with Pulsed Lasers: The Consequences of Hyperfine Structure, Doppler Broadening and Electromagnetically Induced Absorption. *Eur. Phys. J. D* **1998**, *1* (1), 57−70.

(13) Loy, M. M. T. Two-Photon Adiabatic Inversion. *Phys. Rev. Lett.* **1978**, *41* (7), 473−476.

(14) Oberst, M.; Münch, H.; Grigoryan, G.; Halfmann, T. Stark-Chirped Rapid Adiabatic Passage among a Three-State Molecular System: Experimental and Numerical Investigations. *Phys. Rev. A - At. Mol. Opt. Phys.* **2008**, *78* (3), 033409.

(15) Treacy, E. B. Adiabatic Inversion with Light Pulses. *Phys. Lett.* **1968**, *27* (7), 421−422.
(16) Grischkowsky, D.; Loy, M. M. T. Self-Induced Adiabatic Rapid Passage. *Phys. Rev. A* **1975**, *12* (3), 1117−1120.
(17) Vitanov, N. V.; Halfmann, T.; Shore, B. W.; Bergmann, K. Laser-Induced Population Transfer By Adiabatic Passage Techniques. *Annu. Rev. Phys. Chem.* **2001**, *52*, 763−809.
(18) Mukherjee, N.; Zare, R. N. Stark-Induced Adiabatic Raman Passage for Preparing Polarized Molecules. *J. Chem. Phys.* **2011**, *135* (2), 024201.
(19) Perreault, W. E.; Zhou, H.; Mukherjee, N.; Zare, R. N. Harnessing the Power of Adiabatic Curve Crossing to Populate the Highly Vibrationally Excited H_2 (v = 7, j = 0) Level. *Phys. Rev. Lett.* **2020**, *124*, 163202.
(20) Perreault, W. E.; Mukherjee, N.; Zare, R. N. Stark-Induced Adiabatic Raman Passage Examined through the Preparation of D_2 (v = 2, j = 0) and D_2 (v = 2, j = 2, m = 0). *J. Chem. Phys.* **2019**, *150* (23), 234201.
(21) Dong, W.; Mukherjee, N.; Zare, R. N. Optical Preparation of H_2 Rovibrational Levels with Almost Complete Population Transfer. *J. Chem. Phys.* **2013**, *139* (7), 074204.
(22) Perreault, W. E.; Mukherjee, N.; Zare, R. N. Preparation of a Selected High Vibrational Energy Level of Isolated Molecules. *J. Chem. Phys.* **2016**, *145* (15), 154203.
(23) Mukherjee, N.; Perreault, W. E.; Zare, R. N. Stark-Induced Adiabatic Raman Ladder for Preparing Highly Vibrationally Excited Quantum States of Molecular Hydrogen. *J. Phys. B At. Mol. Opt. Phys.* **2017**, *50* (14), 144005.
(24) Bauer, S. H.; Ossa, E. Isotope Exchange Rates. III. The Homogeneous Four-Center Reaction H_2+D_2. *J. Chem. Phys.* **1966**, *45* (2), 434−443.
(25) Herman, I. P. Molecular Hydrogen Exchange: A Study of HD(V = 5)+HD(V = 0)→H_2+D_2. *J. Chem. Phys.* **1980**, *72* (10), 5777−5778.
(26) Bauer, S. H.; Lederman, D. M.; Resler, E. L.; Fisher, E. R. The Homogeneous Gas Phase H_2-D_2 Metathesis at Room Temperature: Reaction Induced by Specific Vibrational Excitation. *Int. J. Chem. Kinet.* **1973**, *5* (1), 93−106.
(27) Brown, N. J.; Silver, D. M. Reactive and Inelastic Scattering of H_2+D_2 Using a Repulsive Model Potential Energy Surface. *J. Chem. Phys.* **1978**, *68* (8), 3607−3617.
(28) Wadehra, J. M.; Bardsley, J. N. Vibrational- and Rotational-State Dependence of Dissociative Attachment in e-H_2 Collisions. *Phys. Rev. Lett.* **1978**, *41* (26), 1795−1798.
(29) Allan, M.; Wong, S. F. Effect of Vibrational and Rotational Exictation on Dissociative Attachment in Hydrogen. *Phys. Rev. Lett.* **1978**, *41* (26), 1791−1794.
(30) Perreault, W. E.; Mukherjee, N.; Zare, R. N. Quantum Control of Molecular Collisions at 1 K. *Science.* **2017**, *358*, 356−359.
(31) Perreault, W. E.; Mukherjee, N.; Zare, R. N. Quantum Controlled Rotationally Inelastic Scattering of HD with H_2 and D_2 near 1 K Reveals Collisional Partner Reorientation. *Nat. Chem.* **2018**, *10*, 561−567.
(32) Zhou, H.; Perreault, W. E.; Mukherjee, N.; Zare, R. N. Shape Resonance Determined from Angular Distribution in D_2 (v = 2, j = 2) + He → D_2 (v = 2, j = 0) + He Cold Scattering. *J. Chem. Phys.* **2021**, *154* (10), 104309.
(33) Fabrikant, I. I.; Wadhera, J. M.; Xu, Y. Resonance Processes in e - H_2 Collisions: Dissociative Attachment and Dissociation from Vibrationally and Rotationally Excited States. *Phys. Scr.* **2002**, *T96*, 45−51.
(34) Horáček, J.; Čížek, M.; Houfek, K.; Kolorenč, P.; Domcke, W. Dissociative Electron Attachment and Vibrational Excitation of H_2 by Low-Energy Electrons: Calculations Based on an Improved Nonlocal Resonance Model. *Phys. Rev. A* **2004**, *70*, 052712.
(35) Gauyacq, J. P. Dissociative Attachment in e^- - H_2 Collisions. *J. Phys. B Atom. Mol. Phys.* **1985**, *18*, 1859.
(36) Orient, O. J.; Chutjian, A. Experimental Study of Dissociative Attachment in H_2: Effect of Vibrational Excitation. *Phys. Rev. A* **1999**, *59* (6), 4374−4378.
(37) Bacal, M.; Wada, M. Negative Ion Source Operation with Deuterium. *Plasma Sources Sci. Technol.* **2020**, *29* (3), 033001.
(38) Berkner, K. H.; Pyle, R. V.; Stearns, J. W. Intense, Mixed-Energy Hydrogen Beams for CTR Injection. *Nucl. Fusion* **1975**, *15* (2), 249−254.
(39) Moir, R. HYLIFE-II Inertial Fusion Energy Power Plant Design. *Fusion Technol.* **1992**, *21*, 1475−1486.
(40) Lovejoy, C.; Nesbitt, D. J. Slit Pulsed Valve for Generation of Long-Path- Length Supersonic Expansions Slit Pulsed Valve for Generation of Long Path-Length Supersonic Expansions. *Rev. Sci. Instrum.* **1987**, *58*, 807−811.
(41) Xu, H.; Chen, G.; Patel, D. N.; Cao, Y.; Ren, L.; Xu, H.; Shao, H.; He, J.; Kim, D. E. Gas Density Distribution in a Clustered-Gas Jet Produced from a Supersonic Slit Nozzle under High Backing Pressure. *AIP Adv.* **2021**, *11* (7), 075313.

https://doi.org/10.1021/acs.jpclett.2c01209
J. Phys. Chem. Lett. 2022, 13, 4682−4687